AUT Journal of Electrical Engineering

AUT J. Elec. Eng., 52(1) (2020) 107-120
DOI: 10.22060/eej.2019.14901.5246

A Robust Control Strategy for Distributed Generations in Islanded Microgrids

Esmaeel Rokrok[1,*], Fariba Shavakhi Zavareh[1], Jafar Soltani[2], Mahmoud Reza Shakarami[1]

[1] Department of Technical & Engineering, Lorestan University, Khorramabad, Iran
[2] Emeritus professor of the Faculty of Electrical and Computer Engineering, Isfahan University of Technology

ABSTRACT: This paper presents a robust control scheme for distributed generations (DGs) in islanded mode operation of a microgrid (MG). In this strategy, assuming a dynamic slack bus with constant voltage magnitude and phase angle, nonlinear equations of the MG are solved in the slack-voltage-oriented synchronous reference frame, and the instantaneous active and reactive power reference for the slack bus is obtained at each time step, based on Y_bus equation of the MG. The slack bus power references are robustly tracked by the proposed adaptive sliding mode based power controller. In addition, a hyper-plan sliding controller is suggested for other DGs that provides three regulators including active power, reactive power and voltage regulator for DG units and ensures protection of the power electronic interfaces to the faults assumed to have occurred in the MG. At each step time, DGs are modeled as positive and negative current sources that are controlled by their adaptive sliding mode controllers in the normal and abnormal operating conditions. All the parameters of controllers are derived via particle swarm optimization (PSO) algorithm in order to minimize an appropriate cost function. Performance of the proposed control strategy is compared to the performance of the conventional master-slave based control strategy. The validity and effectiveness of the presented method are supported by time domain simulation of a test microgrid in MATLAB.

Review History:
Received: 2018-09-04
Revised: 2019-10-04
Accepted: 2019-10-15
Available Online: 2020-06-01

Keywords:
Adaptive control
Dynamic analysis
Islanded mode operation

1. INTRODUCTION

A microgrid (MG) system usually refers to a part of a low- or medium-voltage distribution system, which is comprised of several distributed generators (DGs), a cluster of local loads and energy storage devices [1]. It is very important to control a MG due to its automation in both islanded and grid-connected modes of operation. The most important challenges in MGs protection and control include uncertainties, dynamic modeling and stability; control and reliability issues are more significant in islanded mode [1,2]. Most DGs are based on electronically-interfaced where the primary control shares power and inverts output voltage. The controllers can be developed in dq coordinate (as PI-based controllers), αβ frame (as Proportional-Resonant (PR) controllers), or abc frame (as hysteresis, or dead-beat) [2]. Power sharing control strategies of the DGs can be divided into two categories: droop-based and non-droop-based. The main objective of the primary control irrespective of whether it is droop-based or non-droop-based, is to ensure that the output voltage of the DG is sinusoidal with adjustable magnitudes and phase angles under any loading conditions and faults. In addition, the control strategy must be robust against parameter uncertainties and transitions between islanded and grid-connected modes of the MG [2,3]. In the Droop based method, the DGs participate in adjusting voltage and frequency of the MG, the total active and reactive power demand of the MG is locally shared among DG units without using any communications among them. However, the frequency and voltage of the MG deviate and a complementary control scheme is required to restore frequency and voltage [4–7]. Then, the supervisor should send proper signals through the intercommunication links periodically. Moreover, the power sharing under droop control method highly depends on the impedance of the filter of the interface inverter and impedance of the interlink line. Poor transient performance, the inability for black start up after system collapse and ignoring load dynamics are the other disadvantages of the conventional droop control technique [8–10]. For accurate power sharing and regulating frequency and voltage of the network, a modified droop characteristic is proposed in [11] which is composed of the angle droop, the frequency droop and the changed voltage droop. The combined droop control scheme can decrease the frequency deviation of the network and share the active and the reactive power accurately with appropriate droop coefficients. In [12], an adaptive droop controller has been proposed based on a superimposed frequency in which the power sharing is performed more accurately than the conventional droop method. In this paper, both primary and secondary controllers use local measured parameters without extra communication links, which increases stability and reliability. However, power sharing accuracy is increased by adapting the

*Corresponding author's email: rokrok.e@lu.ac.ir

droop gains that the main drawback is the stability reduction. In [13], a control method has been presented based on combination of the virtual impedance, voltage compensation and droop method for a balanced power sharing among DG units with insignificant frequency and voltage deviations. However, this paper has used the conventional PI controller which should be re-tuned in different conditions and it is not robust and stable. In [14], a multivariable controller design based on droop method has been presented which consists of Cascade, feed-forward and repetitive controllers. The proposed strategy regulates the frequency and voltage of the balanced, unbalanced, and nonlinear loads. However, poor transient response and low stability margin are drawbacks of this control method. The most widely adopted technique of non-droop-based control is the master-slave method, in which, one DG operates as the master unit for adjusting the frequency and voltage magnitude of the network, while the other DGs transfer the pre-defined amount of power [15–19]. In practice, a microgrid should be able to operate under all balanced/unbalanced loading conditions and normal/fault conditions without any performance degradations. In the presence of unbalanced loads or faults, a DG unit must inject a portion of the negative-sequence current to balance the load voltages. A number of control strategies on robust control applications for microgrids have been proposed under undesirable conditions. The $H\infty$ and μ-synthesis robust controls are the linear robust control techniques which provide effective control methods for dynamical systems. But, most linear robust control methods suggest complex statefeedback controllers, whose orders are not smaller than the order of the controlled systems [20-22]. Sliding-mode controller (SMC) is an effective nonlinear robust controller with invariant control effect on internal perturbations and external disturbances if the controlled state trajectory slides along the designed sliding surface [23]. The combination of adaptive control techniques and SMC is established as a beneficial robust technique for MG control with real external disturbances and parametric uncertainties in islanded microgrids under unbalanced loads [23-26]. An adaptive sliding mode controller (SMC) has been proposed in [23] to increase the rejection of external disturbances and internal perturbation to assure robustness of the control system of the inverter. In this work, only the output voltage of the DGs is controlled without considering current amplitude under fault condition. Reference [24] has considered a voltage-control scheme for an islanded MG, based on fractional-order SMC. However, the suggested fractional-order SMC in [24] regulates the terminal voltage of the DG units without controlling the current. Thus, the major problem is the stability. A control strategy has been presented based on SMC in reference [25] for DG units. The recommended control scheme presents a stable and fast control on frequency and voltage of the DGs. However, the negative components of voltage and current are not considered in this control scheme. A recursive fast terminal sliding mode control (FTSMC) has been developed in [26] for a MG system. A voltage controller based on recursive approach of FTSMC has been used to control the bus voltage closer to the upstream grid and farther away from the DG units in a grid-connected MG. Reference [27] has proposed a droop-free strategy that fulfills both the secondary and the primary control aims for an Islanded MG. Active, reactive and voltage controllers use its local and neighbor's data to update information. But, any communication link failure needs instantaneous maintenance before other links fail. Thus, reliability of the system is weak.

Adopting the droop-free characteristic for an autonomous multi-bus MG, the main contribution of this work is to suggest a dynamic slack bus with constant voltage magnitude and phase angle. Nonlinear equations of the MG are solved in the slack-voltage-oriented synchronous reference frame, and the instantaneous active and reactive power references of slack bus are obtained at each time step. Since the amplitude and phase of the slack bus are forced to remain constant, the frequency and voltage of the MG are controlled. An adaptive sliding mode controller is introduced to adjust the active and reactive power quantities which must be provided by the slack bus DG, robustly. Moreover, adaptive hyper-plane sliding mode power controllers are introduced to regulate the output active and reactive power and output voltage of other DGs, robustly. The proposed control scheme is designed to work independently from the network topology, system parameters, and load models of the MG. In section 2, the robust control strategy based on a dynamic slack unit is proposed. An adaptive sliding mode based active power controller and a hyper-plane sliding mode based reactive power controller are developed in section 3. Section 4 represents the simulation results to verify the validity and effectiveness of the presented control methods. Finally, the paper is concluded in section 5.

2. THE PROPOSED VOLTAGE CONTROL FOR SLACK UNIT

In the island mode operation, the DG unit with the highest power rating (DG1) can be operated as a dynamic slack bus. Therefore, the slack unit must generate the required amounts of active and reactive powers such that the voltage magnitude and angle of the slack bus are forced to be constant at their respective references. In the following, the design procedure of the proposed control strategy is explained. Consider a multi-DG grid-connected MG, numbering the DGs terminal buses from 1 to M and remaining buses from M+1 to N (Fig 1.) The loads can be represented by their equivalent impedances. Quasi-static networks are usually described by the admittance matrix of Y_{bus}. Define the vectors:

$$\begin{bmatrix} I_{od}(t) \\ I_{oq}(t) \\ 0 \\ 0 \end{bmatrix} = \begin{bmatrix} \mathrm{Re}\{Y_{GG}\} & -\mathrm{Im}\{Y_{GG}\} & \mathrm{Re}\{Y_{GP}\} & -\mathrm{Im}\{Y_{GP}\} \\ \mathrm{Im}\{Y_{GG}\} & \mathrm{Re}\{Y_{GG}\} & \mathrm{Im}\{Y_{GP}\} & \mathrm{Re}\{Y_{GP}\} \\ \mathrm{Re}\{Y_{PG}\} & -\mathrm{Im}\{Y_{PG}\} & \mathrm{Re}\{Y_{PP}\} & -\mathrm{Im}\{Y_{PP}\} \\ \mathrm{Im}\{Y_{PG}\} & \mathrm{Re}\{Y_{GG}\} & \mathrm{Im}\{Y_{PP}\} & \mathrm{Re}\{Y_{PP}\} \end{bmatrix} \begin{bmatrix} V_{Gd}(t) \\ V_{Gq}(t) \\ V_{Pd}(t) \\ V_{Pq}(t) \end{bmatrix} \quad (1)$$

with

$$V_{Gd}(t) = \left[V_{G1,d}(t) \;\; V_{G2,d}(t) \ldots V_{GM,d}(t) \right]^{T} \quad (2)$$

$$V_{Gq}(t) = \left[V_{G1,q}(t) \;\; V_{G2,q}(t) \ldots V_{GM,q}(t) \right]^{T} \quad (3)$$

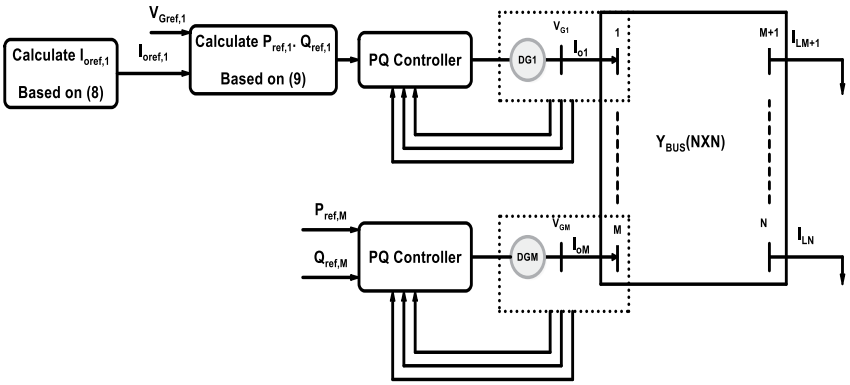

Fig. 1 Islanded microgrid with proposed strategy.

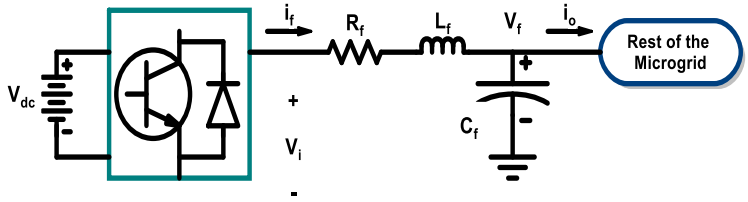

Fig. 2 Model of an inverter-based DG unit.

$$I_{od}(t)=\left[I_{o1,d}(t)\quad I_{o2,d}(t)\ \cdots\ I_{oM,d}(t)\right]^{T} \tag{4}$$

$$I_{oq}(t)=\left[I_{o1,q}(t)\quad I_{o2,q}(t)\ \cdots\ I_{oM,q}(t)\right]^{T} \tag{5}$$

Where V_{Pd} and V_{Pq} are voltages of the load buses and the remaining buses from M+1 to N. At each step time of (Δt), based on network Y_{bus} equations, nonlinear equations of the microgrid are solved in the slack voltage oriented synchronous reference frame and then output voltages of the DGs (vector V_G) are obtained. In transient state conditions of the microgrid, the same as steady state conditions, the first DG unit is assumed to act as a dynamic slack bus with a constant voltage magnitude and reference angle. Considering this assumption, the reference vector V_G^{ref} is derived from V_G such that only the terminal voltage of the slack $(DG1)$ unit is replaced with reference value V_{G1dq}^{ref} :

$$V_G^{ref}=\left[V_{G1dq}^{ref}\ V_{G2,dq}\cdots\ V_{GM,dq}\right]^{T} \tag{6}$$

Based on the obtained V_G^{ref} and considering the matrix equation (1):

$$\begin{bmatrix}V_{Pd}^{ref}(t)\\V_{Pq}^{ref}(t)\end{bmatrix}=-\begin{bmatrix}Re\{Y_{PP}\}&-Im\{Y_{PP}\}\\Im\{Y_{PP}\}&Re\{Y_{PP}\}\end{bmatrix}^{-1} \tag{7}$$
$$\left(\begin{bmatrix}Re\{Y_{PG}\}&-Im\{Y_{PG}\}\\Im\{Y_{PG}\}&Re\{Y_{GG}\}\end{bmatrix}\begin{bmatrix}V_{Gd}^{ref}(t)\\V_{Gq}^{ref}(t)\end{bmatrix}\right)$$

$$\begin{bmatrix}I_{od}^{ref}(t)\\I_{oq}^{ref}(t)\end{bmatrix}=\begin{bmatrix}Re\{Y_{PG}\}&-Im\{Y_{PG}\}\\Im\{Y_{PG}\}&Re\{Y_{GG}\}\end{bmatrix}\begin{bmatrix}V_{Gd}^{ref}(t)\\V_{Gq}^{ref}(t)\end{bmatrix}+ \tag{8}$$
$$\begin{bmatrix}Re\{Y_{PP}\}&-Im\{Y_{PP}\}\\Im\{Y_{PP}\}&Re\{Y_{PP}\}\end{bmatrix}\begin{bmatrix}V_{Pd}^{ref}(t)\\V_{Pq}^{ref}(t)\end{bmatrix}$$

In fact, the matrix equations (7-8) are solved such that terminal voltage of the slack DG unit is forced to keep at its reference value. Then, the reference current of the slack unit (defined by I_{o1dq}^{ref}) is obtained at each step time of Δt, based on (8). The instantaneous active power references of the slack unit are obtained as:

$$\begin{bmatrix}P_1^{ref}\\Q_1^{ref}\end{bmatrix}=\begin{bmatrix}V_{f1d}^{ref}I_{o1d}^{ref}+V_{f1q}^{ref}I_{o1q}^{ref}\\V_{f1q}^{ref}I_{o1d}^{ref}-V_{f1d}^{ref}I_{o1q}^{ref}-\omega_0C_f\{(V_{f1d}^{ref})^2+(V_{f1q}^{ref})^2\}\end{bmatrix} \tag{9}$$

In order to force the voltage magnitude and angle of the slack bus to be constant at their respective commands, an adaptive sliding mode controller is designed for tracking the active and reactive power references that are obtained by the proposed strategy.

3. THE PROPOSED ADAPTIVE SMC FOR DG UNITS

Fig.2 demonstrates an inverter-based DG which consists of a DC power supply, three-phase voltage source converter (VSC) interfaces and a LC filter that is connected to the bus of v_{ok}. Control of the VSC is performed in a rotating

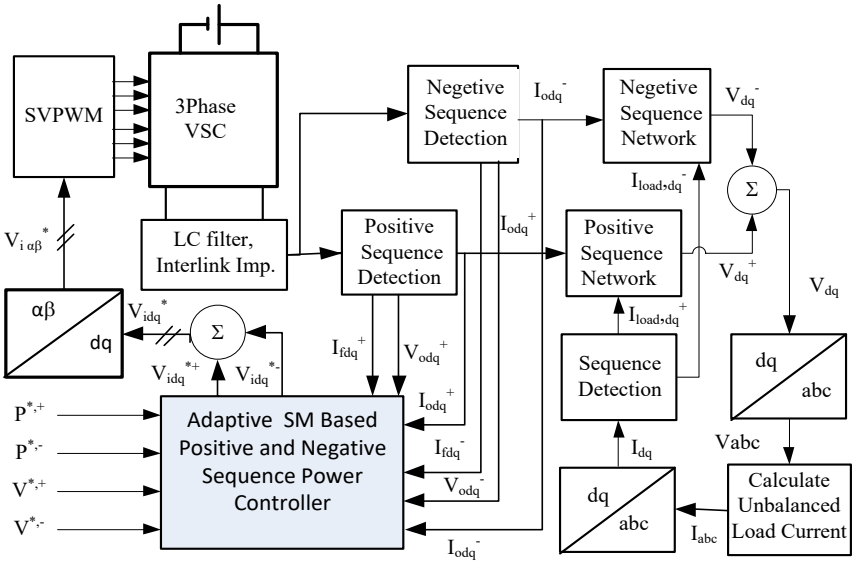

Fig. 3. Block diagram of the proposed analysis method.

reference frame in which the direct and quadrature axes are specified by d and q, respectively. Using the well-known Park transformation, the voltage and current equations in the synchronous rotating frame can be derived as:

$$\frac{di_{fdq}(t)}{dt} = \alpha(v_{idq}(t) - \beta i_{fdq}(t) - v_{fdq}(t)) + \begin{bmatrix} 0 & \omega(t) \\ -\omega(t) & 0 \end{bmatrix} i_{fdq}(t) \quad (10)$$

$$\frac{dv_{fdq}(t)}{dt} = \gamma(i_{fdq}(t) - i_{odq}(t)) + \begin{bmatrix} 0 & \omega(t) \\ -\omega(t) & 0 \end{bmatrix} v_{fdq}(t) \quad (11)$$

where $v_i = \begin{bmatrix} v_{id} & v_{iq} \end{bmatrix}^T, i_f = \begin{bmatrix} i_{fd} & i_{fq} \end{bmatrix}^T$, $v_f = \begin{bmatrix} v_{fd} & v_{fq} \end{bmatrix}^T$, and $i_o = \begin{bmatrix} i_{od} & i_{oq} \end{bmatrix}^T$ are the output voltage of the inverter, current of the filter, output voltage of the DG, and output current if the DG (Fig. 1). Besides, $\frac{1}{L_{fk}}, \beta = R_{fk}, \gamma = \frac{1}{C_{fk}}$ are the nominal parameters of the DG.

The proposed control scheme consists of the positive and negative sequences power controllers as shown in Fig.3. These power controllers are designed to adjust the positive and negative sequences active and reactive powers that are injected to the MG by the DG unit. The active and reactive power references are sent to the power controller that adjusts the output power using a dq0 reference frame rotating with the output voltage of the inverter. If parameters of the filter deviate from their nominal values ($\Delta\alpha$,$\Delta\beta$ and $\Delta\gamma$ respectively), equations (10)-(11) can be modified as:

$$\frac{di_{fdqk}(t)}{dt} = \alpha(v_{idqk}(t) - \beta i_{fdqk}(t) - v_{fdqk}(t)) \pm \omega_0(t) i_{fqdk}(t) + \eta_{dq} \quad (12)$$

$$\frac{dv_{fdqk}(t)}{dt} = \gamma(i_{fdqk}(t) - i_{odqk}(t)) \pm \omega_0(t) v_{fqdk}(t) + \vartheta_{dq} \quad (13)$$

where η_{dq} and ϑ_{dq} are the lumped-sum uncertainties which can be written as:

$$\eta_{dq} = \Delta\alpha\left(v_{idqk}(t) - \beta i_{fdqk}(t) - v_{fdqk}(t)\right) - \Delta\beta(\alpha + \Delta\alpha) i_{fdqk}(t) + \delta_{dq} \quad (14)$$

$$\vartheta_{dq} = \Delta\gamma\left(i_{fdqk}(t) - i_{odqk}(t)\right) + \nu_{dq} \quad (15)$$

where Δ denotes the difference from nominal value and the terms δ_{dq} and ν_{dq} are added to account disturbances and other un-modeled uncertainties for system equations. The instantaneous active and reactive powers injected by the DG unit to the connection bus can be represented as:

$$P_f = \frac{3}{2}\left(v_{fd}(t) i_{fd}(t) + v_{fq}(t) i_{fq}(t)\right) \quad (16)$$

$$Q_f = -\frac{3}{2}\left(v_{fq}(t) i_{fd}(t) - v_{fd}(t) i_{fq}(t)\right) \quad (17)$$

The main control objective for PQ controlled DGs is to adjust the active and reactive power delivered to the MG by the DG. To enhance the transient performance, and to increase the disturbance rejection ability and reference tracking accuracy, an adaptive sliding mode controller based on direct power control strategy is suggested for positive and negative sequence of active and reactive power of all DG units. In order to eliminate the reaching phase and decreasing steady-state errors caused by nonlinear sliding motion, for the active power sliding mode controller, the integral based sliding function is chosen as:

$$S_{Pf} = e_{Pf} + K_{IP} \int_0^t e_{Pf} dt \quad (18)$$

where K_{IP} is positive constant gain and e_{Pf} is the error signal corresponding to the active power of the DG given by

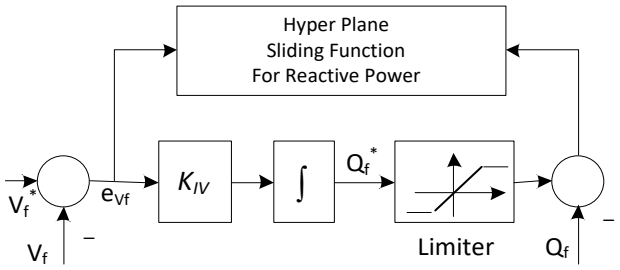

Fig. 4. Reactive power reference realization

$e_{Pf} = P_f^* - P_f$. Based on the sliding mode control, it is required to restrict the controlled state to its corresponding sliding surface. Consider the sliding function (18), Differentiating S_{Pf} yields:

$$\frac{d}{dt}S_{Pf} = \frac{d}{dt}e_{Pf} + K_{IP}e_{Pf} = -\frac{d}{dt}P_f + K_{IP}e_{Pf} \tag{19}$$

In the typical Q control scheme, the reactive power reference might be selected directly (for example, Q* = 0), or might be chosen to provide a pre-defined voltage profile at the inverter output [2]. Stability and robustness of the conventional PI controller are weak against the faults, system uncertainties and unbalanced loads. Therefore it cannot be a desirable candidate for controlling the system. A hyper-plane sliding mode controller is proposed in this paper for the reactive power controller. (i) It does not require to know the online reactive power reference. (ii) The presented controller can force the voltage error towards zero asymptotically and also keep the reactive power bounded. The hyper-plane sliding function is defined as:

$$S_{Qf} = e_{Qf} + e_{vf} + K_{IQ}\int_0^t \left(e_{Qf} + e_{vf}\right)dt \tag{20}$$

where K_{IQ} is positive constant gain and e_{Qf} and e_{vf} are the error signals corresponding to the reactive power and output voltage of the DG given as follows:

$$e_{Qf} = Q_f^* - Q_f, \tag{21}$$

$$e_{vf} = v_f^* - v_f, \quad v_f = \sqrt{\left(v_{fd}^2 + v_{fq}^2\right)} \tag{22}$$

where superscript (*) denotes the reference values. Reactive power reference (Q_f^*) is defined as:

$$Q_f^* = K_{Iv}\int_0^t e_{vf}dt \tag{23}$$

where K_{Iv} is the positive constant gain. Fig. 4 shows building the reference of the reactive power for use in the hyper-plane sliding function.

Based on the sliding control strategy, it is necessary to restrict the controlled state to its corresponding sliding surfaces. Consider the sliding function (20), differentiating S_{Qf}, yields:

$$\frac{d}{dt}S_{Qf} = \frac{d}{dt}e_{Qf} + \frac{d}{dt}e_{vf} + K_{IQ}\left(e_{Qf} + e_{vf}\right) \tag{24}$$

where:

Another step is to define a control law so that $S = [S_{Pf}\ S_{Qf}]^T$ leads to zero and is sustained thereafter. The aim is to design a desirable control law, u, such that the sliding functions (18) and (20) satisfy

$$\begin{bmatrix}\frac{d}{dt}S_{Pf}\\ \frac{d}{dt}S_{Qf}\end{bmatrix} = 0 \tag{25}$$

Considering (19), (24) and (12-17), it can be shown that (appendix A):

$$\begin{aligned}\frac{d}{dt}\begin{bmatrix}S_{Pf}\\ S_{Qf}\end{bmatrix} &= -A\begin{bmatrix}i_{fd}\\ i_{fq}\end{bmatrix} - \begin{bmatrix}v_{fd} & v_{fq}\\ v_{fq} & -v_{fd}\end{bmatrix}B - \frac{3}{2}\begin{bmatrix}v_{fd} & v_{fq}\\ v_{fq} & -v_{fd}\end{bmatrix}\begin{bmatrix}\alpha v_{id}\\ \alpha v_{iq}\end{bmatrix}\\ &- \begin{bmatrix}0\\ \frac{d}{dt}v_f\end{bmatrix} + \begin{bmatrix}K_{IP} & 0\\ 0 & K_{IQ}\end{bmatrix}\begin{bmatrix}e_{Pf}\\ e_{Qf}\end{bmatrix}\\ &+ \begin{bmatrix}0\\ K_{Iv} + K_{IQ}\end{bmatrix}e_{vf} - \frac{3}{2}\begin{bmatrix}\eta_d & \eta_q\\ \eta_q & -\eta_d\end{bmatrix}\begin{bmatrix}i_{fd}\\ i_{fq}\end{bmatrix} - \frac{3}{2}\begin{bmatrix}v_{fd} & v_{fq}\\ v_{fq} & -v_{fd}\end{bmatrix}\begin{bmatrix}\vartheta_d\\ \vartheta_q\end{bmatrix}\end{aligned} \tag{26}$$

$$A = \frac{3}{2}\begin{bmatrix}\gamma(i_{fd} - i_{od}) + \omega_0 v_{fq} & \gamma(i_{fq} - i_{oq}) - \omega_0 v_{fd}\\ \gamma(i_{fq} - i_{oq}) - \omega_0 v_{fd} & -\gamma(i_{fd} - i_{od}) - \omega_0 v_{fq}\end{bmatrix} \tag{27}$$

$$B = \frac{3}{2}\begin{bmatrix}\alpha(-v_{fd} - \beta i_{fd}) + \omega_0 i_{fq}\\ \alpha(-v_{fq} - \beta i_{fq}) - \omega_0 i_{fd}\end{bmatrix} \tag{28}$$

$$\begin{aligned}\frac{d}{dt}v_f &= \frac{2v_{fd}\frac{dv_{fd}}{dt} + 2v_{fq}\frac{dv_{fq}}{dt}}{2\sqrt{v_{fd}^2 + v_{fq}^2}}\\ &= \frac{1}{\sqrt{v_{fd}^2 + v_{fq}^2}}\Big(v_{fd}\left(\gamma(i_{fd} - i_{od}) + \omega_0 v_{fq} + \vartheta_d\right) +\\ &v_{fq}\left(\gamma(i_{fq} - i_{oq}) - \omega_0 v_{fd} + \vartheta_q\right)\Big)\end{aligned} \tag{29}$$

$$\frac{d}{dt}v_f = \frac{1}{\sqrt{v_{fd}^2 + v_{fq}^2}}\begin{bmatrix}v_{fd} & v_{fq}\end{bmatrix}\left(\begin{bmatrix}\gamma(i_{fd} - i_{od}) + \omega_0 v_{fq}\\ \gamma(i_{fq} - i_{oq}) - \omega_0 v_{fd}\end{bmatrix} + \begin{bmatrix}\vartheta_d\\ \vartheta_q\end{bmatrix}\right) \tag{30}$$

The modified control law is considered to be

$$u = \begin{bmatrix} v_{id} & v_{iq} \end{bmatrix}^T = u_{ao} + u_{as} = \begin{bmatrix} v_{ido} & v_{iqo} \end{bmatrix}^T + \begin{bmatrix} v_{ids} & v_{iqs} \end{bmatrix}^T \quad (31)$$

where u_{ao} is used for the nominal system and u_{as} deals with the system parameter variations and the external disturbances [23],[28-29]. First, it is assumed that $S=0,\ \dot{S}=0$. Considering nominal values of the parameters, the equivalent SMC can be obtained by setting equation (26) to zero and selecting u_{ao} as follows:

$$u_{ao} = \begin{bmatrix} v_{ido} \\ v_{iqo} \end{bmatrix} = \frac{2}{3\alpha} \begin{bmatrix} v_{fd} & v_{fq} \\ v_{fq} & -v_{fd} \end{bmatrix}^{-1} \left\{ -A \begin{bmatrix} i_{fd} \\ i_{fq} \end{bmatrix} - \begin{bmatrix} v_{fd} & v_{fq} \\ v_{fq} & -v_{fd} \end{bmatrix} B - \begin{bmatrix} 0 & 0 \\ v_{fd} & v_{fq} \end{bmatrix} C_v + \begin{bmatrix} K_{IP} & 0 \\ 0 & K_{IQ} \end{bmatrix} \begin{bmatrix} e_{Pf} \\ e_{Qf} \end{bmatrix} + \begin{bmatrix} 0 \\ K_{Iv} + K_{IQ} \end{bmatrix} e_{vf} \right\} \quad (32)$$

$$C_v = \frac{1}{\sqrt{v_{fd}^2 + v_{fq}^2}} \begin{bmatrix} \gamma(i_{fd} - i_{od}) + \omega_0 v_{fq} \\ \gamma(i_{fq} - i_{oq}) - \omega_0 v_{fd} \end{bmatrix} = \frac{1}{v_f} \begin{bmatrix} \gamma(i_{fd} - i_{od}) + \omega_0 v_{fq} \\ \gamma(i_{fq} - i_{oq}) - \omega_0 v_{fd} \end{bmatrix} \quad (33)$$

Considering uncertainties of the DG model, the controller designed in (32) is combined with adaptive term so that robust behavior is obtained from the developed closed-loop system. Clearly, if real parameters of the model are not equal to the nominal values, then $\dot{S} \neq 0$ and the system response will not settle on the sliding-surface. Considering equation (26), derivative of the sliding-surface can be written as:

$$\dot{S} = \dot{S}_n - \mu_s \quad (34)$$

$$\dot{S}_n = -A \begin{bmatrix} i_{fd} \\ i_{fq} \end{bmatrix} - \begin{bmatrix} v_{fd} & v_{fq} \\ v_{fq} & -v_{fd} \end{bmatrix} B - \frac{3}{2} \begin{bmatrix} v_{fd} & v_{fq} \\ v_{fq} & -v_{fd} \end{bmatrix} \begin{bmatrix} \alpha v_{id} \\ \alpha v_{iq} \end{bmatrix} + \begin{bmatrix} K_{IP} & 0 \\ 0 & K_{IQ} \end{bmatrix} \begin{bmatrix} e_{Pf} \\ e_{Qf} \end{bmatrix} + \begin{bmatrix} 0 \\ K_{Iv} + K_{IQ} \end{bmatrix} e_{vf} \quad (35)$$

$$\mu_s = \frac{3}{2} \begin{bmatrix} \eta_d & \eta_q \\ \eta_q & -\eta_d \end{bmatrix} \begin{bmatrix} i_{fd} \\ i_{fq} \end{bmatrix} + \frac{3}{2} \begin{bmatrix} v_{fd} & v_{fq} \\ v_{fq} & -v_{fd} \end{bmatrix} \begin{bmatrix} \vartheta_d \\ \vartheta_q \end{bmatrix} + \frac{1}{v_f} \begin{bmatrix} 0 & 0 \\ v_{fd} & v_{fq} \end{bmatrix} \begin{bmatrix} \vartheta_d \\ \vartheta_q \end{bmatrix} \quad (36)$$

where, S_n is the sliding-surface for the nominal parameters while all of the system uncertainties are expressed by μ_s. Clearly, on the sliding-surface, $S_n = S = 0$. In this paper, corresponding to the lumped uncertainty given in (36), the adaptive term u_{as} is modified as [28-29]:

$$u_{as} = \begin{bmatrix} v_{ids} \\ v_{iqs} \end{bmatrix} = \frac{2}{3\alpha} \begin{bmatrix} v_{fd} & v_{fq} \\ v_{fq} & -v_{fd} \end{bmatrix}^{-1} \left\{ \hat{\Gamma} \mathrm{sgn}(S) \right\} \quad (37)$$

where, $\hat{\Gamma}$ is an adjustable gain constant. In order to keep the trajectory on the sliding surface, size of the uncertainties should be bounded. Assume that there exists a positive number Γ_d such that:

$u_{as} = \begin{bmatrix} v_{ids} \\ v_{iqs} \end{bmatrix} = \frac{2}{3\alpha} \begin{bmatrix} v_{fd} & v_{fq} \\ v_{fq} & -v_{fd} \end{bmatrix}^{-1} \{ \Gamma_d \mathrm{sgn}(S) \}$ is a terminal solution for u_{as}, where Γ_d must satisfy $\Gamma_d > |\mu_s|$. If the adaptive law is chosen as:

$$\frac{d}{dt}\hat{\Gamma} = \gamma_s^{-1}.S \quad (38)$$

where γ_s is a diagonal matrix, in which the diagonal entries are positive adaption gains. In addition, by selecting an appropriate adaptation gain γ_s, high control activity in the reaching mode can be prevented effectively. As an illustration, one may also define γ_s to be a function of S and make it vary before the sliding surface is achieved. Define the adaption error as $\tilde{\Gamma} = \hat{\Gamma} - \Gamma_d$. In order to prove the stability of the adaptive sliding control law for the inverters operating in the islanded MG, a Lyapunov function is defined as follows:

$$V = \frac{1}{2} S^T S + \frac{1}{2} \tilde{\Gamma}^T \gamma_s \tilde{\Gamma} \quad (39)$$

Differentiating V with respect to time yields:

$$\frac{d}{dt}V = S^T \left(\frac{d}{dt}S\right) + \tilde{\Gamma}^T \gamma_s \left(\frac{d}{dt}\tilde{\Gamma}\right) \quad (40)$$

Considering (27), it can be acquired that:

$$\frac{d}{dt}V = S^T(-\mu_s - \hat{\Gamma}\mathrm{sgn}(S)) + (\hat{\Gamma} - \Gamma_d)^T \gamma_s \left(\frac{d}{dt}\hat{\Gamma}\right) \quad (41)$$

Then

$$\frac{d}{dt}V = S^T\left(-\mu_s - \hat{\Gamma}\mathrm{sgn}(S)\right) + (\hat{\Gamma} - \Gamma_d)^T \gamma_s (\gamma_s^{-1}|S|) = -S^T\mu_s - S^T\hat{\Gamma}\mathrm{sgn}(S) + S^T\mathrm{sgn}(S)\left(\hat{\Gamma} - \Gamma_d\right) = -S^T\mu_s - \Gamma_d|S| < 0 \quad (42)$$

Because the time-derivative of the Lyapunov function, V, is negative definite, the suggested voltage control strategy is asymptotically stable. Both S and $\tilde{\Gamma}$ reach zero in finite time, i.e., $S \to 0$ and $\hat{\Gamma} \to \Gamma_d$ Therefore, $e_{Pf} \to 0$, $e_{Qf} \to 0$ and $e_{vf} \to 0$ can be proved through definition of the sliding surfaces in (18) and (20). Thus, the convergence of the adaptive gain parameter $\tilde{\Gamma}$ and the reaching of sliding mode, as well as the tracking control can be guaranteed [28]. It can be assumed that the commanded voltage $u = u_{ao} + u_{as}$ seems at the input of the filter inductor i.e. $\left(u_{ao} + u_{as} = v_{idqo} + v_{idqs} = v_{idqk}\right)$. Under fault condition, voltage of the DG drops, therefore, power controller increases current of the DG in response to the voltage drop. For over-current protection, the active and reactive power references should be limited as a function of the actual output voltage amplitude of the DG. Based on the maximum output current of the DG, I_{max}, and the active and reactive power references, the minimum amplitude of the voltage of the DG, V_{min}, can be obtained as:

$$V_{min} = \frac{\sqrt{P_{ref}^2 + Q_{ref}^2}}{I_{max}} \quad (43)$$

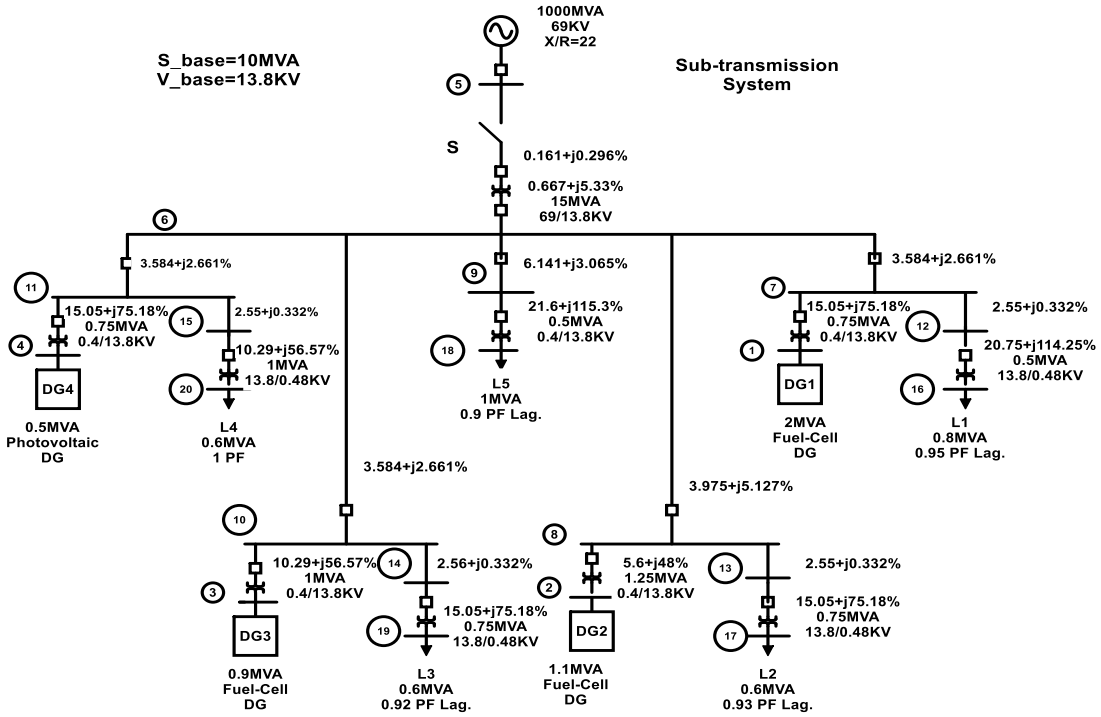

Fig. 5. The considered microgrid.

If $V_f < V_{min}$, the reactive power delivered by the DG unit should be limited to:

$$Q_{max} = V_f I_{max} \sin\varphi \qquad \varphi = \tan^{-1}\left(\frac{Q_{ref}}{P_{ref}}\right) \tag{44}$$

Based on (44), a dynamic limiter can be designed for Q_{ref} to ensure that output current of the converter is within the allowable limits (see Fig. 4). Therefore, the over-current protection of the converter can be easily ensured in case that voltage of the DG drops.

The tunable parameters in the designed sliding functions are K_{IP}, K_{IQ} , K_{IV} and Γ_d , where the selected parameters are searched by using the PSO algorithm in given parameter spaces under normal condition. The cost function in the PSO algorithm is critical for the searching performance [29]. In this paper, a quantitative performance index based on the sum of the absolute active power, reactive power and voltage deviations is adopted as the cosy function, which is:

$$J(t) = \sum_{i=1}^{n} \int_0^{t_1} \left(\left|e_{Pfi}\right|^2 + \left|e_{Qfi}\right|^2 + \left|e_{Vfi}\right|^2 \right) dt \tag{45}$$

where n is the number of the DGs, and $t1$ is the total simulation time. Smaller cost value indicates better control performance. The number of the optimized parameters is 3n, and the optimized parameter set is $K = [K_{IP1}, K_{IQ1}, K_{IV1}, \Gamma_{d1} \ldots, K_{IP4}, K_{IQ4}, K_{IV4}, \Gamma_{d4}]$.

According to the investigation of related work and design experience, the searching ranges of these parameters are set as $K_{IP} = [1000; 10000], K_{IQ} = [1000; 10000], \Gamma_d = [1e3; 2e3]$and $K_{IV} = [0; 20]$. The number of the particles and the initial maximum velocity are chosen as 20 and 10% of the searching upper limit corresponding to each parameter. For the *j*th particle in the *i*th generation, the particle updates its velocity and location by using the following equations

$$v_{ij}(t+1) = w(t)\, v_{ij}(t) + c_1\left(pbest - x_{ij}(t)\right) + c_2\left(gbest - x_{ij}(t)\right) \tag{46}$$

$$x_{ij}(t+1) = x_{ij}(t) + v_{ij}(t+1) \tag{47}$$

where $x_{ij}(t)$ and $v_{ij}(t)$ represent the location and the velocity at time t, pbest expresses the local best location, and gbest is the global best location. $w(t)$ is the learning rate from the initial value 0.9 decreasing to the final value 0.4. By minimizing the cost function $J(t)$ over time, the algorithm can obtain the optimal parameters [29].

4. SIMULATION RESULTS

In order to verify effectiveness of the suggested control scheme, the test autonomous MG system shown in Fig.5 is simulated in MATLAB. Moreover, the performance of the proposed control strategy is compared with the master slave control strategy represented in [25] to demonstrate effectiveness of the dynamic slack strategy. Of course, the only master unit (DG1) employs voltage mode conventional SMC based controller of [25] while the rest of the controllers use the proposed adaptive based controller. In the proposed control strategy, the DG1 employs the same adaptive power controller as the other units. Parameters of the DGs and its controller

Table 1. DG parameters and its controller gains.

System parameters	Symbol	values
Grid voltage	V_{s-rms}	13.8 KV
Fundamental frequency	f_s	50 Hz
DC bus voltage	V_{dc}	700V
Filter resistance	R_f	0.012 Ω
Filter inductance	L_f	800 µH
Filter capacitance	C_f	320 µF
Switching frequency	f_{sw}	6480 Hz
Active power controller gain	K_{Ip}	8135
Reactive power controller gain	K_{IQ}	9433
Voltage controller gain	K_{IV}	13
Uncertainty upper bound constant	Γ_d	1379

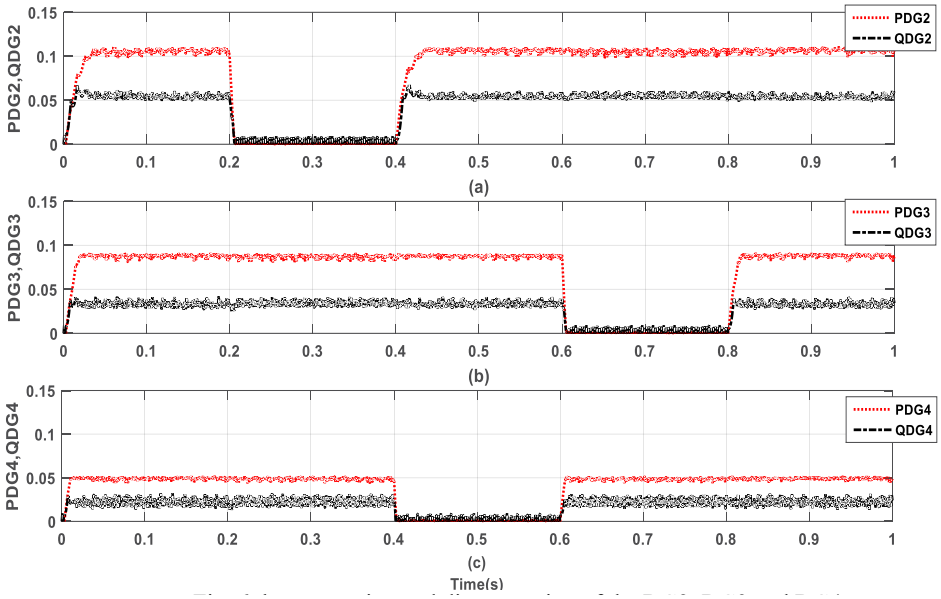

Fig. 6. the connection and disconnection of the DG2, DG3 and DG4.

gains are given in Table 1. The initial steady state condition of the MG is obtained by means of AC load flow analysis. For any scenario that occurs in the MG system, the nonlinear differential equations of the system are solved by means of MATLAB code. Two types of load are considered for evaluating effectiveness of the presented control strategy; (1) balanced linear loads, (2) unbalanced linear loads. The balanced loads are connected through 13.8/0.48 kV transformers and consist of three star-connected series RL loads. The unbalanced load is constructed through a 13.8/0.48 kV transformer that consists of a series RL load between phase-a and the neutral conductor and its two other phases are open. The load inductance and resistance are 40 µH and 30 mΩ, respectively.

4.1. Connection and disconnection of DG2, DG3 and DG4

In order to force the magnitude and phase angle of the slack bus voltage to be constant at the respective command, the slack bus power references are robustly tracked by the proposed adaptive sliding mode based power controller. This case illustrates the responses of the system to stepwise changes in their active power commands both with the proposed control strategy and the master slave strategy. At first, the microgrid operates in the autonomous mode but, the active power references of all DG units are set to their rated values. In this case, DGs generate enough reactive power to maintain their voltage in the reference value of the microgrid. Fig. 6, Fig. 7 and Fig. 8 show active, reactive power and output voltages of DGs with the connection and disconnection of DG2, DG3 and DG4. As Fig 6 shows at t = 0.2s, the DG2 is disconneted from respective bus. At t = 0.4s, the DG4 is disconnected from the MG and the DG2 is conneted to the MG. At t = 0.6s, the active power references of DG2, DG3 and DG4 are set to $P_{ref2} = 0.11pu$, $P_{ref3} = 0.0pu$ and $P_{ref4} = 0.05pu$. Finally, at t = 0.8s, the active power references of all of DGs are set to the respective command. Fig. 7 illustrates response of the DG1 to connection and disconnetion of DG2, DG3 and DG4 using the proposed control strategy and the master slave strategy. As Fig 7 shows output power of DG1 increases after

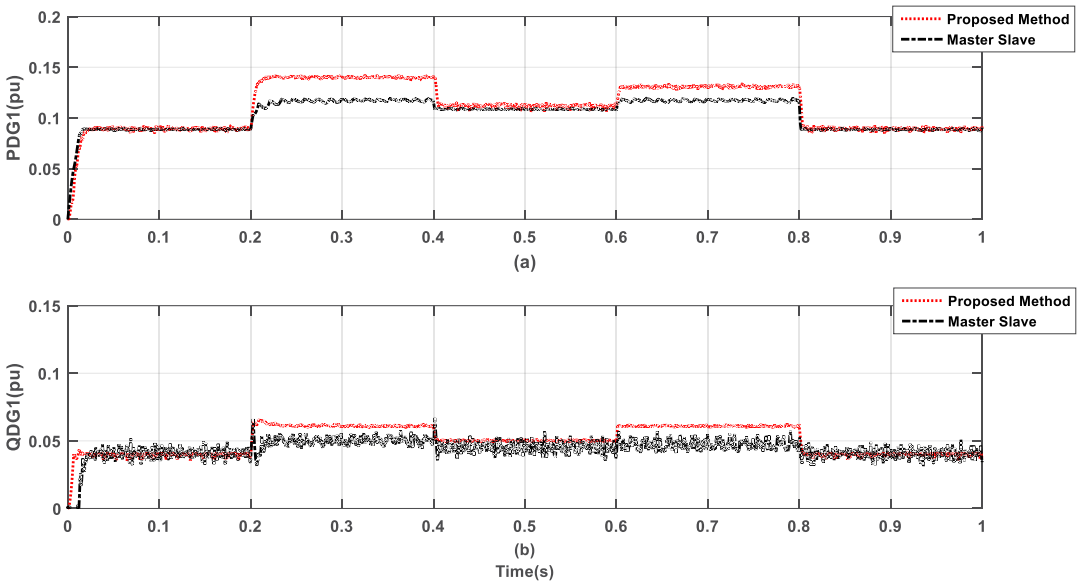

Fig. 7. Responses of the DG1 to the connection and disconnection of the DGs

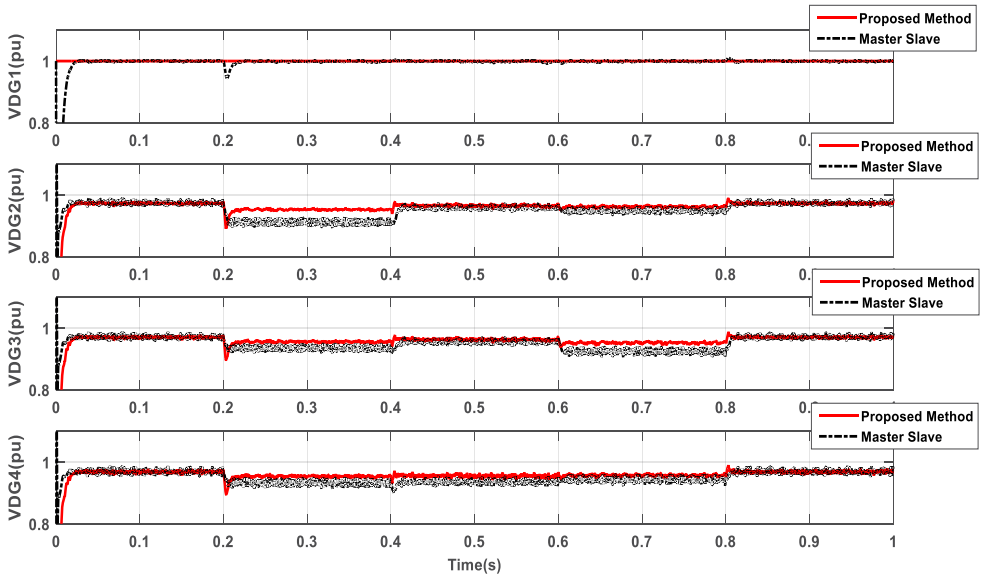

Fig. 8. The DGs voltages with the connection and disconnection of the DG2, DG3 and DG4

disconnection of DG2, DG3 and DG4. Fig 8 shows the slack voltage (DG1) is set to 1 p.u. and the other voltages of the DGs are ramped to 0.98 p.u. It can be seen that the output powers of the DGs track their corresponding commands resulting in changes in the connection and disconnection of the DGs. It should be noted that the active and reactive power of the slack bus (DG1) is changed in order to force the voltage amplitude and phase of the slack bus to be constant. On the other hand, the reactive power references of all DGs are changed based on the hyperplane sliding mode controller in order to adjust the output voltage of the DGs flexibly. Fig. 7 and Fig. 8 illustrste the proposed method has better voltage control and operates faster and more accurately than the master slave method with more active and reactive power generation.

4.2. The system response to a single phase to ground fault

This simulation shows the performance of the MG system under the single phase to ground fault, in an islanded MG (switch S is opened). In this case, at first, all DG units are connected to the MG and active powers are set to references value and reactive power references are flexible. At t =0.1s, a fault occurs in middle of the transmission line between buses 6 and 9 and at t= 0.2s, the fault is cleared. Fig. 9 demonstrates performance of the MG to the fault. As shown in Fig 9(a), under this fault, the proposed adaptive controller is able to maintain the output voltage of the DG units at their corresponding references. Fig 9 (b-d) also shows that the active and reactive powers of the DG unit track their corresponding references.

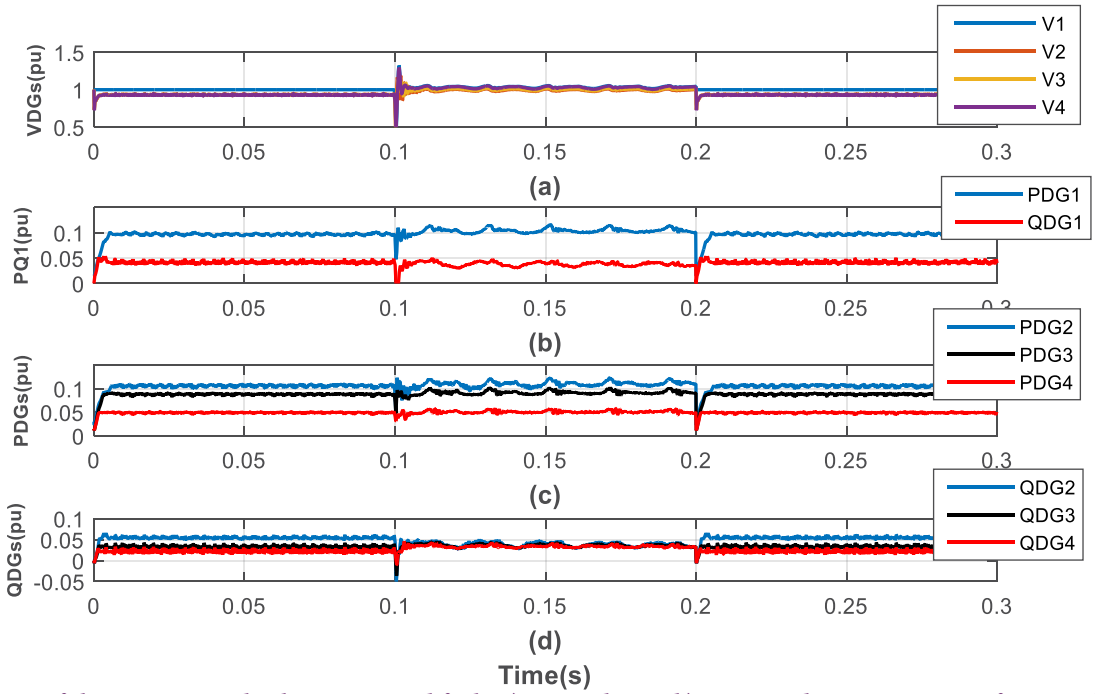

Fig. 9. Responses of the MG to a single phase to ground fault. a) DGs voltages. b) Active and reactive powers of DG1. c-d) Active and reactive Powers of DGs respectively.

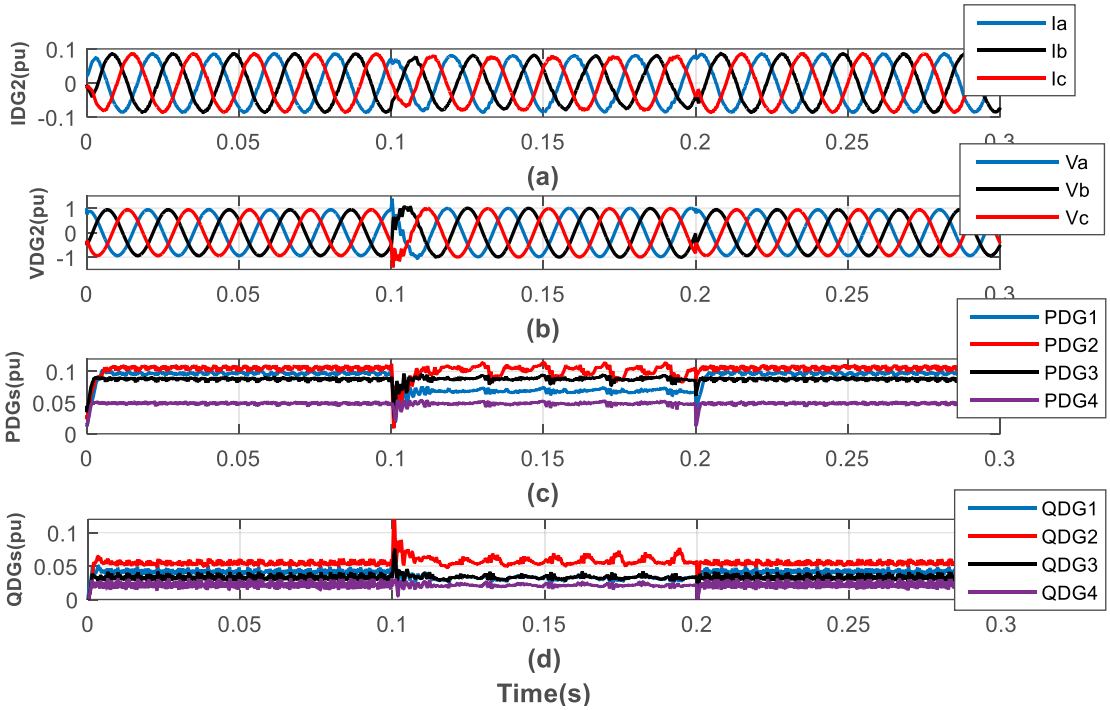

Fig. 10. System responses to unbalanced load. a) DG2 cuurent. b) DG2 voltage. c-d) Active and reactive Powers of DGs respectively.

4.3. Response to unbalanced load

In this case, the MG system is initially started under balanced condition, then an unbalanced load is added to bus 17 and bus 18 at t = 0.1s. The unbalanced load is made up of a series RL load between phase-a bus 17 to ground and phase-b bus 18 to ground; inductance and resistance of the load are $L = 40\mu H$ and $R = 30m\Omega$. Fig. 10 illustrates response of the MG to the unbalanced loading. It can be seen that the output powers of the DGs track their respective references, resulting in corresponding changes in the reactive power of the DGs. The active power reference of DG2, DG3 and DG4 are constant, but the reactive power references are flexible in order to hold the voltage constant. The active power of the DGs follow their reference values. However, under an

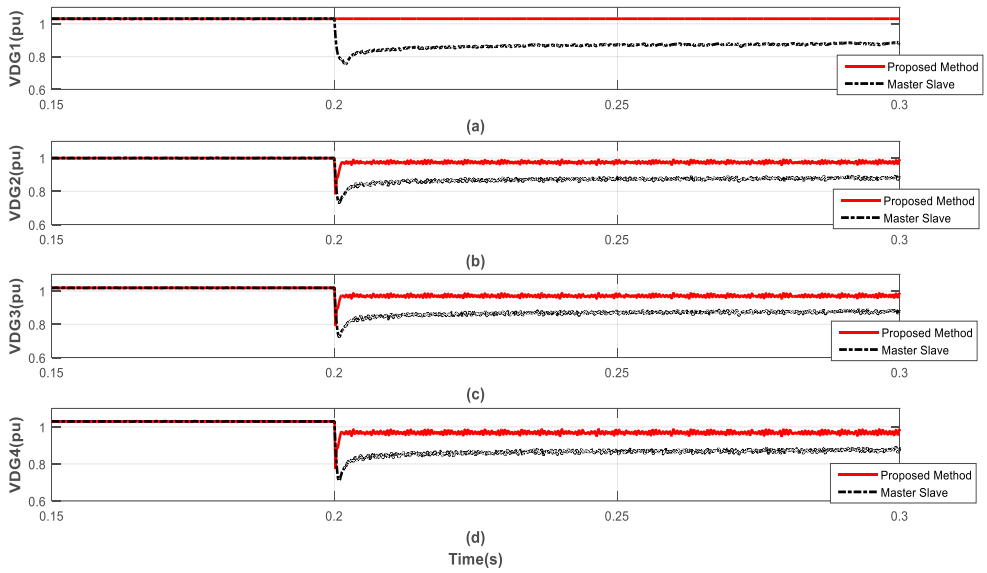

Fig. 11. Responses of the MG, transferring between grid-connected and islanded modes

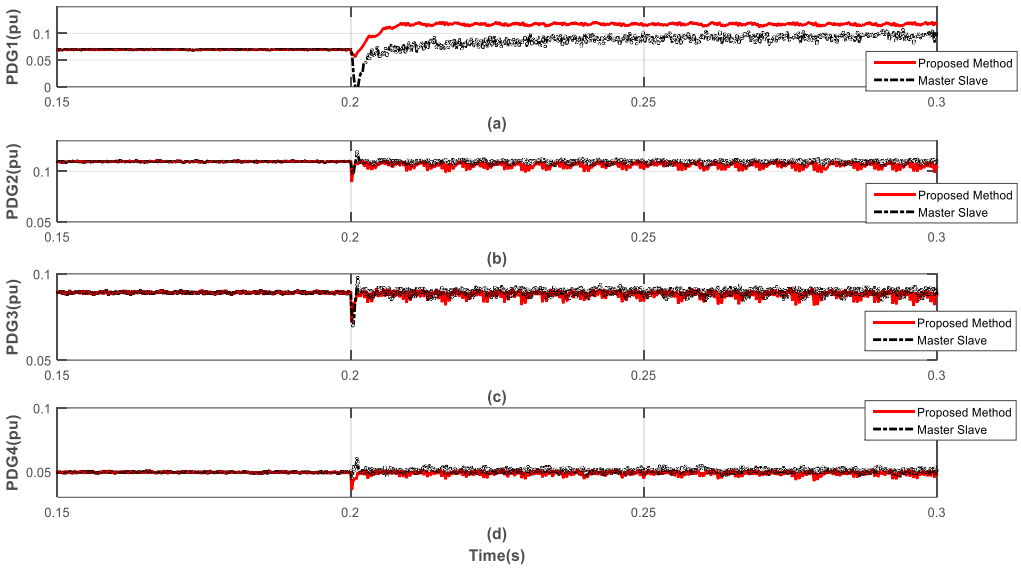

Fig. 12. Responses of the MG , transferring between grid-connected and islanded modes

unbalanced condition, the instantaneous active and reactive power of the DGs experience double frequency oscillations. The output reactive powers of the DGs change further under this condition in order to maintain the output voltages and finally settles on new values. In order to evaluate robustness of the recommended controllers subject to parametric uncertainties, a 50% mismatch is considered for resistances and inductors of the filters from $R_f = 0.012\Omega$ and $L_f = 24\mu H$ to $R_f = 1.5 \times 0.012\Omega$ and $L_f = 0.5 \times 24\mu H$ at $t = 0.25s$. Fig. 10 illustrates that the output voltages and currents of the DG units track their respective commands. A comparison between before and after mismatches illustrates that there is no considerable difference between the two responses.

4.4. Transferring between grid-connected and islanding modes

This simulation illustrates performance of the suggested control scheme in transitions from grid-connected mode to islanded mode of the MG. In this study, at first, switch S is closed. Therefore, the MG operates in the grid-connected mode and active references of DGs are set to their reference value, respectively. At t = 0.2s, the switch S is opened and the MG system operates in islanded mode. Fig .11 and Fig. 12 show performance of the proposed strategy compared maste slave strategy for these transferring. Figure 11 shows that the proposed method is more accurate and faster than the m and has a more robust operation.

5. CONCLUSIONS

This paper proposes an adaptive control scheme for autonomous operation of a multi-bus microgrid comprising several inverter-based DGs. Assuming a dynamic slack bus with a constant voltage magnitude and phase angle, the instantaneous active and reactive power components of the slack bus are obtained at each step time based on node equations of the microgrid. In order to obligate the voltage magnitude and angle of the slack bus to be constant at their corresponding commands, the obtained power components as the slack bus power references are tracked on-line by the proposed adaptive sliding mode based power controller. The lumped uncertainties imposed on the DG unit power dynamic, involving disturbances and DG parameter changes, are estimated through an adaptive algorithm. Moreover, a hyper-plane sliding mode controller is designed for the rest of the DG units that regulate active, reactive and terminal voltages of DGs. Performance of the proposed adaptive strategy under normal and faulted conditions, balanced and unbalanced load and parameter uncertainties are demonstrated through time-domain simulation and compared with the performance of a control strategy presented in [25]. The proposed controller is stable and robust against the unbalanced loads, faults and uncertainties of the system.

REFERENCES

[1] B.F.o. H. Bevrani, and T. Ise, Microgrid Dynamics and Control, Wiley, 2017.

[2] D.E. Olivares, A. Mehrizi-Sani, A.H. Etemadi, C.A. Cañizares, R. Iravani, M. Kazerani, A.H. Hajimiragha, O. Gomis-Bellmunt, M. Saeedifard, R. Palma-Behnke, Trends in microgrid control, IEEE Transactions on smart grid, 5(4) (2014) 1905-1919.

[3] X. Zhang, J. Liu, T. Liu, L. Zhou, A novel power distribution strategy for parallel inverters in islanded mode microgrid, in: 2010 Twenty-Fifth Annual IEEE Applied Power Electronics Conference and Exposition (APEC), IEEE, 2010, pp. 2116-2120.

[4] M.B. Delghavi, A. Yazdani, Islanded-mode control of electronically coupled distributed-resource units under unbalanced and nonlinear load conditions, IEEE Transactions on Power Delivery, 26(2) (2010) 661-673.

[5] H. Karimi, H. Nikkhajoei, R. Iravani, Control of an electronically-coupled distributed resource unit subsequent to an islanding event, IEEE Transactions on Power Delivery, 23(1) (2007) 493-501.

[6] M.N. Marwali, A. Keyhani, Control of distributed generation systems-Part I: Voltages and currents control, IEEE Transactions on power electronics, 19(6) (2004) 1541-1550.

[7] A. Elrayyah, Y. Sozer, M. Elbuluk, A novel load flow analysis for particle-swarm optimized microgrid power sharing, in: 2013 Twenty-Eighth Annual IEEE Applied Power Electronics Conference and Exposition (APEC), IEEE, 2013, pp. 297-302.

[8] J.C. Vasquez, J.M. Guerrero, M. Savaghebi, J. Eloy-Garcia, R. Teodorescu, Modeling, analysis, and design of stationary-reference-frame droop-controlled parallel three-phase voltage source inverters, IEEE Transactions on Industrial Electronics, 60(4) (2012) 1271-1280.

[9] S.M. Ashabani, Y.A.-R.I. Mohamed, General interface for power management of micro-grids using nonlinear cooperative droop control, IEEE Transactions on Power Systems, 28(3) (2013) 2929-2941

[10] M. Babazadeh, H. Karimi, A robust two-degree-of-freedom control strategy for an islanded microgrid, IEEE transactions on power delivery, 28(3) (2013) 1339-1347.

[11] Y. Xia, Y. Peng, W. Wei, Triple droop control method for ac microgrids, IET Power Electronics, 10(13) (2017) 1705-1713.

[12] S. Peyghami, H. Mokhtari, F. Blaabjerg, Decentralized load sharing in a low-voltage direct current microgrid with an adaptive droop approach based on a superimposed frequency, IEEE Journal of Emerging and Selected Topics in Power Electronics, 5(3) (2017) 1205-1215.

[13] A. Ketabi, S.S. Rajamand, M. Shahidehpour, Power sharing in parallel inverters with different types of loads, IET Generation, Transmission & Distribution, 11(10) (2017) 2438-2447.

[14] S. Gholami, M. Aldeen, S. Saha, Control strategy for dispatchable distributed energy resources in islanded microgrids, IEEE Transactions on Power Systems, 33(1) (2017) 141-152.

[15] J.P. Lopes, C. Moreira, A. Madureira, Defining control strategies for microgrids islanded operation, IEEE Transactions on power systems, 21(2) (2006) 916-924.

[16] M.M. Rezaei, J. Soltani, Robust control of an islanded multi-bus microgrid based on input–output feedback linearisation and sliding mode control, IET Generation, Transmission & Distribution, 9(15) (2015) 2447-2454.

[17] B. Zhao, X. Zhang, J. Chen, Integrated microgrid laboratory system, IEEE Transactions on power systems, 27(4) (2012) 2175-2185.

[18] S.-W. Lee, B.-H. Cho, Master–slave based hierarchical control for a small power DC-distributed microgrid system with a storage device, Energies, 9(11) (2016) 880.

[19] A. Mortezaei, M.G. Simões, M. Savaghebi, J.M. Guerrero, A. Al-Durra, Cooperative control of multi-master–slave islanded microgrid with power quality enhancement based on conservative power theory, IEEE transactions on smart grid, 9(4) (2016) 2964-2975.

[20] A. Kahrobaeian, Y.A.-R.I. Mohamed, Direct Single-Loop/spl mu/-Synthesis Voltage Control for Suppression of Multiple Resonances in Microgrids with Power-Factor Correction Capacitors, IEEE Transactions on Smart Grid, 4(2) (2013) 1151-1161.

[21] P. Li, Z. Yin, Y. Li, The realization of flexible photovoltaic power grid-connection μ-synthesis robust control in microgrid, in: 2014 IEEE PES General Meeting| Conference & Exposition, IEEE, 2014, pp. 1-5.

[22] H. Bevrani, M.R. Feizi, S. Ataee, Robust Frequency Control in an Islanded Microgrid: H∞ and μ-Synthesis Approaches, IEEE transactions on smart grid, 7(2) (2015) 706-717.

[23] Z. Chen, A. Luo, H. Wang, Y. Chen, M. Li, Y. Huang, Adaptive sliding-mode voltage control for inverter operating in islanded mode in microgrid, International Journal of Electrical Power & Energy Systems, 66 (2015) 133-143.

[24] M.B. Delghavi, S. Shoja-Majidabad, A. Yazdani, Fractional-order sliding-mode control of islanded distributed energy resource systems, IEEE Transactions on Sustainable Energy, 7(4) (2016) 1482-1491.

[25] M.B. Delghavi, A. Yazdani, Sliding-mode control of AC voltages and currents of dispatchable distributed energy resources in master-slave-organized inverter-based microgrids, IEEE Transactions on Smart Grid, 10(1) (2017) 980-991.

[26] V. Nasirian, Q. Shafiee, J.M. Guerrero, F.L. Lewis, A. Davoudi, Droop-free distributed control for AC microgrids, IEEE Transactions on Power Electronics, 31(2) (2015) 1600-1617.

[27] S.K. Gudey, R. Gupta, Recursive fast terminal sliding mode control in voltage source inverter for a low-voltage microgrid system, IET Generation, Transmission & Distribution, 10(7) (2016) 1536-1543.

[28] J. Fei, C. Lu, Adaptive sliding mode control of dynamic systems using double loop recurrent neural network structure, IEEE transactions on neural networks and learning systems, 29(4) (2017) 1275-1286.

[29] Y. Tang, P. Ju, H. He, C. Qin, F. Wu, Optimized control of DFIG-based wind generation using sensitivity analysis and particle swarm optimization, IEEE Transactions on Smart Grid, 4(1) (2013) 509-520.

Appendix A

$$\frac{d}{dt}S_{Pf} = \frac{d}{dt}e_{Pf} + K_{IP}e_{Pf} = -\frac{d}{dt}P_f + K_{IP}e_{Pf} = 0 \tag{A-1}$$

$$\frac{dP_f}{dt} = \frac{3}{2}\left(\frac{dv_{fd}}{dt}i_{fd} + v_{fd}\frac{di_{fd}}{dt} + \frac{dv_{fq}}{dt}i_{fq} + v_{fq}\frac{di_{fq}}{dt}\right) \tag{A-2}$$

$$\frac{dP_f}{dt} = A_P\begin{bmatrix} i_{fd} \\ i_{fq} \end{bmatrix} + \begin{bmatrix} v_{fd} & v_{fq} \end{bmatrix}B_P + \frac{3}{2}\begin{bmatrix} v_{fd} & v_{fq} \end{bmatrix}\begin{bmatrix} \alpha v_{id} \\ \alpha v_{iq} \end{bmatrix} + \mu_{sP} \tag{A-3}$$

$$A_P = \frac{3}{2}\begin{bmatrix} \gamma(i_{fd} - i_{od}) + \omega_0 v_{fq} & \gamma(i_{fq} - i_{oq}) - \omega_0 v_{fd} \end{bmatrix} \tag{A-4}$$

$$B_P = \frac{3}{2}\begin{bmatrix} \alpha(-v_{fd} - \beta i_{fd}) + \omega_0 i_{fq} \\ \alpha(-v_{fq} - \beta i_{fq}) - \omega_0 i_{fd} \end{bmatrix} \tag{A-5}$$

$$\mu_{sP} = \frac{3}{2}\begin{bmatrix} \eta_d & \eta_q \end{bmatrix}\begin{bmatrix} i_{fd} \\ i_{fq} \end{bmatrix} + \frac{3}{2}\begin{bmatrix} v_{fd} & v_{fq} \end{bmatrix}\begin{bmatrix} \vartheta_d \\ \vartheta_q \end{bmatrix} \tag{A-6}$$

$$\frac{d}{dt}S_{Pf} = -\left(A_P\begin{bmatrix} i_{fd} \\ i_{fq} \end{bmatrix} + \begin{bmatrix} v_{fd} & v_{fq} \end{bmatrix}B_P + \frac{3}{2}\begin{bmatrix} v_{fd} & v_{fq} \end{bmatrix}\begin{bmatrix} \alpha v_{id} \\ \alpha v_{iq} \end{bmatrix} + \mu_{sP}\right) + K_{IP}e_{Pf} \tag{A-7}$$

Reactive power derevative:

$$\frac{dQ_f}{dt} = \frac{3}{2}\left(\frac{dv_{fq}}{dt}i_{fd} + v_{fq}\frac{di_{fd}}{dt} - \frac{dv_{fd}}{dt}i_{fq} - v_{fd}\frac{di_{fd}}{dt}\right) \tag{A-8}$$

$$\frac{dQ_f}{dt} = A_Q\begin{bmatrix} i_{fd} \\ i_{fq} \end{bmatrix} + \begin{bmatrix} v_{fq} & -v_{fd} \end{bmatrix}B_Q + \frac{3}{2}\begin{bmatrix} v_{fq} & -v_{fd} \end{bmatrix}\begin{bmatrix} \alpha v_{id} \\ \alpha v_{iq} \end{bmatrix} + \mu_{sQ} \tag{A-9}$$

$$\frac{dv_f}{dt} = \frac{\left(\frac{dv_{fd}}{dt}v_{fd} + \frac{dv_{fq}}{dt}v_{fq}\right)}{\sqrt{v_{fd}^2 + v_{fq}^2}} = \begin{bmatrix} v_{fq} & -v_{fd} \end{bmatrix}C_v \tag{A-10}$$

$$A_Q = \frac{3}{2}\begin{bmatrix} \gamma(i_{fq} - i_{oq}) - \omega_0 v_{fd} & -\gamma(i_{fd} - i_{od}) - \omega_0 v_{fq} \end{bmatrix} \tag{A-11}$$

$$B_Q = \frac{3}{2}\begin{bmatrix} \alpha(-v_{fd} - \beta i_{fd}) + \omega_0 i_{fq} \\ \alpha(-v_{fq} - \beta i_{fq}) - \omega_0 i_{fd} \end{bmatrix} = B_P \tag{A-12}$$

$$C_v = \frac{1}{\sqrt{v_{fd}^2 + v_{fq}^2}}\begin{bmatrix} \gamma(i_{fq} - i_{oq}) - \omega_0 v_{fd} \\ -\gamma(i_{fd} - i_{od}) - \omega_0 v_{fq} \end{bmatrix} = \frac{2/3}{\sqrt{v_{fd}^2 + v_{fq}^2}}A_Q^T \tag{A-13}$$

$$\mu_{sQ} = \frac{3}{2}\begin{bmatrix} \eta_q & -\eta_d \end{bmatrix}\begin{bmatrix} i_{fd} \\ i_{fq} \end{bmatrix} + \frac{3}{2}\begin{bmatrix} v_{fq} & -v_{fd} \end{bmatrix}\begin{bmatrix} \vartheta_d \\ \vartheta_q \end{bmatrix} \tag{A-14}$$

$$\frac{d}{dt}S_{Qf} = -A_Q\begin{bmatrix} i_{fd} \\ i_{fq} \end{bmatrix} - \begin{bmatrix} v_{fq} & -v_{fd} \end{bmatrix}B_Q - \frac{3}{2}\begin{bmatrix} v_{fq} & -v_{fd} \end{bmatrix}\begin{bmatrix} \alpha v_{id} \\ \alpha v_{iq} \end{bmatrix} - \mu_{sQ} - \begin{bmatrix} v_{fq} & -v_{fd} \end{bmatrix}C_v + (K_{IQ} + K_{Iv})e_{vf} + K_{IQ}e_{Qf} \tag{A-15}$$

HOW TO CITE THIS ARTICLE

E. Rokrok, F. Shavakhi Zavareh, J. Soltani, M.R. Shakarami, A Robust Control Strategy for Distributed Generations in Islanded Microgrids, AUT J. Elec. Eng., 52(1) (2020) 107-120.

DOI: 10.22060/eej.2019.14901.5246